IIETA International Information and Engineering Technology Association
Advancing the World of Information and Engineering

Journal of New Materials for Electrochemical Systems
Vol. 27, No. 3, September 2024, pp. 199-207
Journal homepage: http://iieta.org/journals/jnmes

Amelioration of Membraneless Microbial Fuel Cell Performance using Covalently Bonded Yeast with Multi Walled Carbon Nanotube Biocatalyst

Aynul Rifaya. M[1], Venkatesa Prabhu Sundramurthy[2,3]*, Shine Kadaikunnan[4], and Jamal M. Khaled[4]

[1]Department of Chemical Engineering, ÉrodeSengunthar Engineering College, Érode, India
[2]Department of Biotechnology, Faculty of Engineering, Karpagam Academy of Higher Education, Coimbatore 641 021, Tamil Nadu, India
[3]Centre for Natural Products and Functional Foods, Karpagam Academy of Higher Education, Coimbatore 641 021, Tamil Nadu, India
[4]Department of Botany and Microbiology, College of Science, King Saud University, P. O. Box 2455, Riyadh 11451, Saudi Arabia

Corresponding Author Email:haiitsvp@gmail.com

https://doi.org/10.14447/jnmes.v27i3.a05

Received: 15/01/2024
Accepted: 05/08/2024

Keywords:
Carbon nanoparticle; Membraneless; Microbial fuel cell; Nicotinamide Adenine Dinucleotide; Yeast cell.

ABSTRACT

In the present study, a microbial catalyst has been developed for use in membraneless microbial fuel cells (MFCs) by employing yeast e and carbon nanoparticles. A series of characterizations were carried out to investigate the stability, performance, and catalytic activity of MFC. Based on the characterizations, the catalyst demonstrated the outstanding catalytic activity and a considerable maximum power density (MPD) of 352 mW·m-2. This was accomplished by means of reactions involving cytochrome c, cytochrome a3, NAD, and FAD that efficiently transfer electrons. The outcome suggested that yeast adoption leads to significant improvement in MFC performance and catalytic activity. In addition, after eight days, the MPD remains at 85% of its initial value, demonstrating outstanding stability in the MFC.

1. INTRODUCTION

An MFC is an electrochemical device that turns the "microbial reducing power" that micro-organisms create as they break down organic and inorganic substances into electrical energy that humans may use [1], [2], [3], [4]. Recently, MFC system gains more interested because of its inexpensive price, user-friendliness, and ability to directly transform organic resources into electrical energy. Nevertheless, the reason for its limited use is mostly due to its subpar performance. However, extracellular electron transfer (EET) from active cells to the surface ofthe electrode is a key factor that significantly limits performance MFC the [5], [6], [7], [8], [9].Electron transfer can be engagedby microorganisms through one of three types mechanisms: (i) direct electron transfer (DET), which occurs inside the microorganism; (ii) EET with the help of external mediators, such as artificial ones; or (iii) EET with the help of endogenous mediators, which are produced by the microorganism itself [10], [11], [12], [13]. Because of their high toxicity, exogenous mediators, like potassium ferricyanide were shown to be not effective. Nevertheless, one potential solution to these problems is to engineered DET into the microorganisms.

Based on their cell wall, prokaryotic and eukaryotic microbes are classified as different species. Prokaryotic microbes that are known to transport electrons *via* outer membrane cytochromes include Aeromonas hydrophila, Geobactermetallireducens, Shewanella putrefaciens, and Rhadoferraxferrireducens. It is well-known how they transport electrons and that they are catalytic [14], [15], [16]. In previous study, many eukaryotic microbes, such as yeasts of the *Arxulaadeninivorans*, *Saccharomyces cerevisiae* family, *Candida melibiosica* and *Hansenula polymorpha*, have undergone examination of their catalytic activity and electron transport mechanism [17], [18], [19], [20]. Reports suggested that the yeast cells grown from *Saccharomyces cerevisiae* have been proven as a bioelectrochemical catalyst as anodes for MFC because of they are nonpathogenic, inexpensive, easy to mass-produce, and can grow on a wide variety of substrates [21], [22]. Regardless, studies on yeast cell MFCs have come to a standstill because of a performance issue, namely a low max power density (MPD).

In this work, immobilized yeast cells using carbon nanoparticles (MWCNTs) were employed as an anchor material. In biofuel cells, MWCNTs have found extensive application as a support material for biocatalysts. The flocculation process has been traditionally used to immobilize yeast on MWCNT[22]. Yeast cells immobilized on MWCNT have not been widely used as MFC catalysts up to now. The research showed that yeast cells immobilized on MWCNTs served as a dispersion for the MWCNTs after they were released into the electrolyte. Additionally, rather than a membraneless system, they utilized MEA to separate the two chambers.

That led to the development of a novel idea called a "yeast cell-immobilized MWCNT" (yeast/MWCNT), where hydrophobic contact and covalent bonding were crucial in facilitating electron transport. More specifically, the hydrophobic interaction between MWCNT and yeast cells allows for quick electron transport from the cells to the electrode surface [23], [24]. In addition to the hydrophobic contact, yeast

amine groups and MWCNT establish a strong C-N link by covalent bonding [25], [26].

Yeast cell immobilization on a supporting material was also examined in relation to entrapping polymer (EP) and crosslinkers. For the two components to cling well to negatively charged yeast cells, the EP needs to be positively charged. The choice of poly(ethylenimine) (PEI) for this purpose was based on its positive charge characteristic [27]. Glutaraldehyde (GA) is a cross-linker because it facilitates the cross-linking of yeast cells and PEI molecules, which results in polymerization [28]. Additionally, low mixing spin was utilized continuously during the process to preserve the yeast cells. The anode electrode of membraneless MFC is based on a catalytic structure derived from yeast cells. Previously, it was believed that the cathode electrode would also be based on laccase [29].

After experimenting with different catalysts, such as laccase for the cathodic agent, yeast/MWCNT and GA/[yeast/MWCNT/PEI] for the anodic agent, and the optimal yeast-based catalytic structure for the cathodic agent, the stability and performance of membraneless MFCs were evaluated. By utilizing X-ray photoelectron spectroscopy (XPS), the chemical structures of GA/[yeast/MWCNT/PEI] catalysts, yeast/MWCNT, and bare MWCNTwere ascertained. To evaluate the catalyst's catalytic activity, electrochemical characterizations were employed, which include cyclic voltammography (CV) and electrochemical impedance spectroscopy (EIS).

Consequently, the following conclusions about the study's originality were supported by the analysis. Initially, it was proposed that yeast cells and MWCNT may form a structure by hydrophobic contact; this construct would then be used as an anodic catalyst for membraneless MFC. Looking over the literature, it appears that the yeast/MWCNT structure being examined for MFC has not been often described. Additionally, yeast-based catalysts using GA as a crosslinker and PEIhave been proven for better MFC performance. Fabrication of biocatalyst incorporating yeast cells using PEI and crosslinker has been very rarely attempted. Hence, the benchmark methods for evaluating the molecular composition and catalytic activity of membraneless MFC catalysts derived from yeast. Additionally, a membraneless MFC system was suggested that has great performance and stability. Studies like this should help advance the field of research into yeast-based membraneless MFCs.

2. EXPERIMENTAL METHODOLOGY

2.1. Preparation of *Saccharomyces cerevisiae*

An experiment was conducted in which 0.15g of dehydrated *Saccharomyces cerevisiae* were refined in 200 mL of 0.01 M phosphate buffered saline (PBS)(pH 7.5). The medium used for the experiment consisted of yeast extract–peptone–dextrose, which contained yeast extract, peptone, and Dglucose, among other ingredients [30], [31]. For three days in an oxygen-free environment, the culture was spun at 120 rpm. During the course of the cultivation period, the dry biomass was determined by drying and weighing 1 mL of culture every six hours. The yeast growth rate (μ) was determined by measuring the dry biomass [32]. One way to determine when to mix an aliquot of yeast with MWCNT was to look at the yeast's growth rate curve.

2.2. Manufacture for anode catalysts

In the present work, the yeast/MWCNT catalyst was prepared by mixing 1.5 milliliter of yeast aliquot with 6 milligrams per milliliter of MWCNT and spinning the mixture at 50 revolutions per minute for 12 hours. In order to remove residual glucose, the filtrate was rinsed with deionized water after being spun at 8,000 rpm for 7 min. To make catalytic ink, the yeast/MWCNT catalyst was mixed with a 0.01 M PBS buffer solution with a pH of 7.5.

The catalyst composed of GA, yeast, MWCNT, and PEI was made by soaking 5 $mg \cdot mL^{-1}$ of MWCNT in a 3.0 mg/mL poly(ethylenimine) solution for one hour. The MWCNT/PEIcombination was spun in a centrifuge at 10,000 rpm for five minutes. To eliminate any surplus of PEI, deionized water was employed. The next step was to immerse the yeast in a mixture of 1 mL of MWCNT/PEI for 10 hours. Further, the filtrate was washed with deionized water after being spun at 12,000 rpm for 5 minutes in order to extract glucose. After combining the yeast, MWCNT, and PEI, it was necessary to wait three hours before adding a cross-linker and a 0.6% w/v GA solution. The GA/[yeast/MWCNT/PEI] catalyst was rinsed with a PBS buffer solution of pH 3.2 to remove excess GA and prevent excessive crosslinking with yeast cells. The catalyst composed of GA/[yeast/MWCNT/ PEI)] was finished.

A laccase-based catalyst can be made, tested electrochemically, and the yeast growth rate can be measured experimentally.

3.RESULTS AND DISCUSSION

3.1. Yeast cell Production

Under isothermal circumstances, the yeast cell's dry weight was measured at regular intervals (every 6 h) until the concentration reached saturation (Fig. 1). The yeast cell's dryweight increased from 1.42 to 2.35 mg·mL-1 as time went on, and its maximum specific growth rate (μ_{max}) was 0.018 h^{-1}.

Yeast metabolism occurred during culture on a substrate of glucose. Initially, the medium contained 5.5 $mg \cdot mL^{-1}$ of glucose. Since yeast cell proliferation ceased upon depletion of glucose, glucose yields on yeast biomass ($Y_{x/glu}$) were derived by connecting the initial glucose concentration with the ultimate dry biomass obtained in the batch. The result was obtained as 0.48 $mg_{dw} \cdot mg_{glu}^{-1}$ after the computation. The formation of acceptable bonds among yeast, PEI, and GA, as well as the accuracy of the chemical form of the matching catalysts, must be carefully calculated. Figure 2 shows the results of the XPS measurements taken for this purpose.

Additionally, the amount of glucose was determined that the yeast cellsutilized for its growth. The glucose intake rate (R_{glu}) was calculated as 0.035 $mg_{glu} \cdot mg_{dw}^{-1}$ using μ_{max} and $Y_{x/glu}$. After 48 hours, the optimal timing for combining the yeast aliquot with MWCNT was reached. Yeast biomass in aliquot achieved appropriate point when time came and the cells began to end exponential phase.

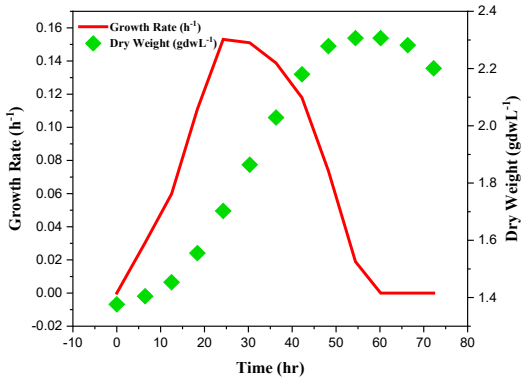

Figure 1. Growth profile of *Saccharomyces cerevisiae*

3.2. Analysis of yeast-based catalytic structures for optimal performance

Figure 2 and 3 display the findings of XPS evaluated for the C1s as well as N1s peaks of the relevant substances, respectively, which provided further proof regarding the creation of the bonds. The only bonds shown by the bare MWCNT catalyst in relation to the XPS C1s peak (Fig. 2a-c) were C=C (sp2) bonds. It was cleared from this C=C bond peak that the MWCNT did not include any functional groups; hence, it was pure. Yeast cells utilize lipids or amino acids to build C-C (sp3) bonds. Then, amines, amides, or N-linked oligosaccharides form C-N bonds. Lastly, O-linked oligosaccharides form C-O bonds [32]. However, new peaks for C-O, C=O, C-N, and C=C bonds emerged while the C=C (sp2) bond peak shrank with the yeast/MWCNT catalyst. Therefore, the C=C bond of MWCNT will most likely be disrupted when yeast cells are combined with it. Once yeast cells have established C-N or C=N connections, they can attach surface amine, amide, or N-linked oligosaccharides with liquid ligands. Observing the C-N (C=N) bond peak validates the correct binding of MWCNTs to yeast cells. Bonding between O-linked oligosaccharide structures was the most probable origin of C-O or C=O connections, whereas the lipid or amino acid on the yeast cell MWCNT is believed to provide a C-C (sp3) bond. The hypothesis that PEI introduces a C-N (C=N) bond peak was disproven because the GA/[yeast/MWCNT/PEI] catalyst exhibited identical peaks to the yeast/MWCNT sample. A C-N or C=N bond can be generated from the C-C bond that yeast creates when the C=C link is broken by interacting with the amine group of PEI, as previously mentioned. The C-N (C=N) bond intensity is higher in GA/[yeast/MWCNT/PEI] compared to yeast/MWCNT, due to the presence of many amine groups in PEI. The C=O and C-N (C=N) bond peaks aren't the only ones that show up when using GA. These peaks are strongly linked to the use of GA.

The absence of XPS N1s peaks in bare MWCNT catalysts (Fig. 3a-c) indicates that they did not include any C-N or C=N bonds. The catalysts made of yeast and MWCNT, as well as GA and [yeast/MWCNT/PEI], exhibited C=N, C-N, and C-N+ bond peaks. It is possible that the yeast and MWCNT complex contained amines, amides, or N-linked oligosaccharides if C=N, C-N, or C-N+ bond peaks were present. Peaks for C=N, C-N, or C-N+ bonds in the GA/[yeast/MWCNT/PEI] mixture indicate a relationship between the amine groups of PEI and MWCNT, or between PEI and yeast. In fact, it proves without a reasonable doubt that the two catalysts produce nitrogen bonds correctly.

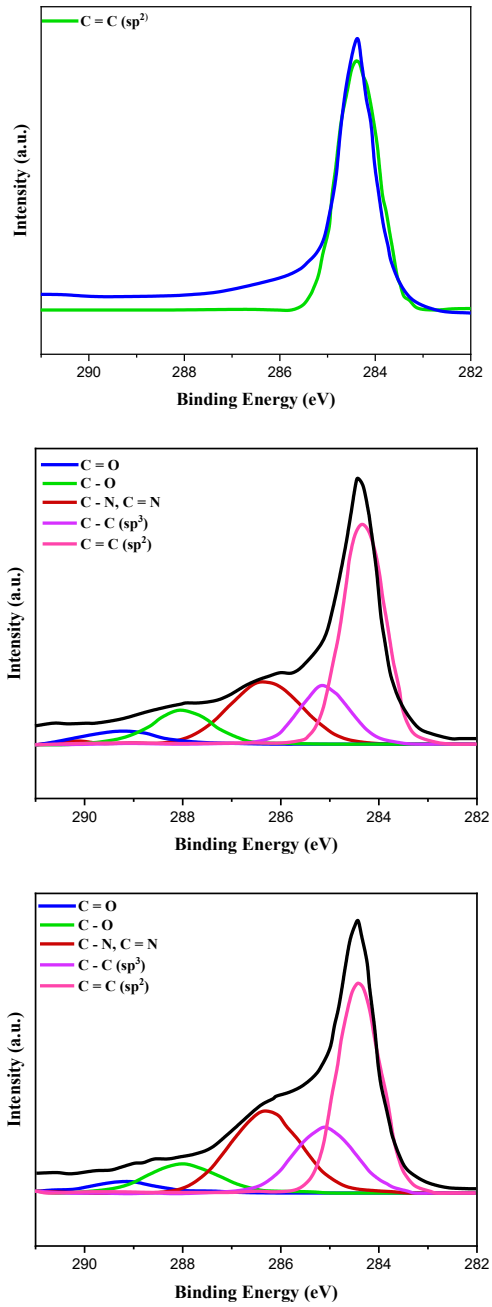

Figure 2. C 1s XPS spectrum of (a) bare MWCNT, (b) yeast/MWCNT and (c) GA/[yeast/MWCNT/PEI] catalysts

The XPS results show that the C-N bond is the most important bond in the yeast/MWCNT catalyst, and that the hydrophobic interaction between the MWCNT and the yeast cell can bring about electron transfer as well. Electric fields generated by GA crosslinking attract positively charged PEI to negatively charged yeast cells, forming the primary bonding mechanism of the GA/[yeast/MWCNT/PEI] catalyst.

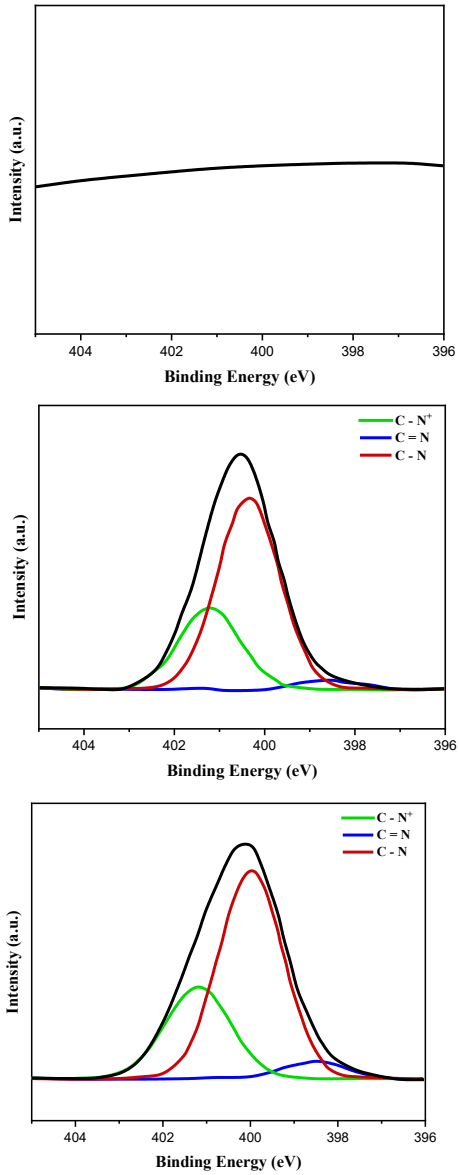

Figure 3. N 1s XPS spectrum of (a) bare MWCNT, (b) yeast/MWCNT and (c) GA/[yeast/MWCNT/PEI] catalysts.

The electrochemical characterizations of the catalyst architectures were used for investigating their catalytic activity. The electrolyte used in the CV testing was 0.01M PBS with a pH of 7.4, and the potential scanning rate was 100 $mV \cdot s_{-1}$. Both the N_2-state and the air-state CV curves were used to determine the intracellular catalytic activity of the yeast. In the N_2-state, the yeast/MWCNT catalyst's CV curve is shown in Fig. 4a. One oxidation peak was observed at 0.3 V vs. Ag/AgCl, whereas two sets of redox peaks were observed at -0.6 and 0.2 V vs. Ag/AgCl, respectively. A peak was seen at 0.2 V vs Ag/AgCl for the cytochrome a3 oxidation reaction and the nicotinamide adenine dinucleotide (NAD) reaction, where $NAD^+ + H_+ + 2e^- \rightarrow NADH$.

As shown in Figure 5, the redox peaks of NAD and cytochrome c~a3 in the yeast/MWCNT structure were validated and confirmed by comparing them to the peaks of bare MWCNT

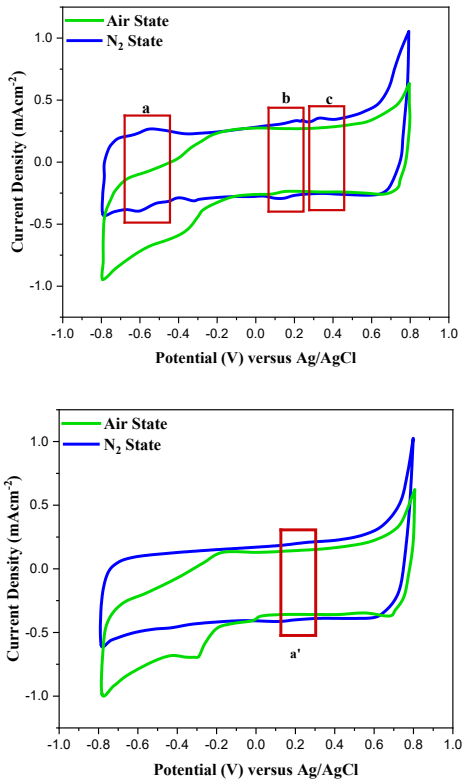

Figure 4. Valuation of yeast/MWCNT and GA/[yeast/MWCNT/PEI] catalysts under air and N_2 conditions of operation, correspondingly.

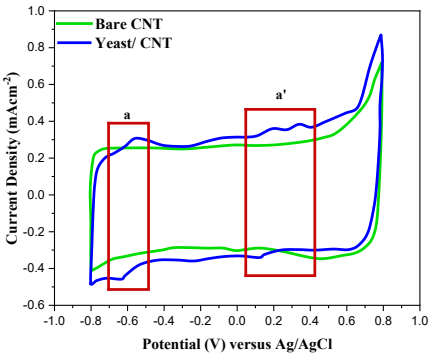

Figure 5. Anaerobic (N_2-state) cyclic voltammograms of yeast/MWCNT (blue solid line) and bare MWCNT (green line).

. The CV tests utilized under a potential scan rate of 100 mV/s and an electrolyte of 0.01M PBS with a pH of 7.5.The absence of redox peaks in the yeast-based catalyst (boxes a and a') suggests that the peaks observed were caused by redox reactions involving NAD, cytochrome c, and cytochrome a3, and not by MWCNT contaminants.

Extracellular electron transfer facilitates the reduction of NAD to NADH during the initial phase of glycolysis (conversion of glucose to pyruvate; -0.6 V against Ag/AgCl). This is evident from a closer inspection of the reaction peaks. If these events occur too frequently, the NAD/NADH coupling could undergo an auto-redox reaction. In the redox reactions of NAD and FAD, electrons produced in the inner Kreb's cycle—which comprises

the cytoplasm and mitochondrial membrane—are transported to the surface of the electrodes [33].

In mitochondria, Kreb's cycle reduction activities help convert NAD to NADH and FAD to $FADH_2$. These processes generate the electrons required for the subsequent stage of the redox reaction connecting cytochrome c (Fe^{3+}) + e^- to cytochrome c (Fe^{2+}) at 0.2 V versus Ag/AgCl. This shift from the ferric-ion to the non-ferric-ion state of cytochrome a3 was shown by the interaction between 0.4 V and Ag/AgCl. [12, 13]. As the process progresses, electrons are transferred to the electrode surface via a hydrophobic interaction that forms between the outer shell of the yeast and the hydrophobic surface of the MWCNT. This interaction is known as the electron route. Figure 5 shows the carbon-to-hydrogen ratio (CV) of the GA/[yeast/MWCNT/PEI] catalyst in solution. When plotted against Ag/AgCl at 0.2 V, only a single pair of tiny redox peaks were visible, in contrast to Fig. 5. The cytochrome c redox process (box a') is responsible for this peak, as previously stated. The oxidation of cytochrome a3 and the NAD redox reaction did not show any peaks. That leads one to believe that the introduction of "PEI and GA" into the mix with "yeast and MWCNT" hinders the ability of the live microbe (the yeast cell) to carry out electron transfer metabolism as intended. This also renders the yeast cell structurally inactive by preventing glycolysis and Kreb's cycle from taking place within the cell. Deactivated yeast cells are unable to transport electrons and stop generating them through redox processes involving NADH and $FADH_2$. Hydrophobic interaction induces a higher level of electron transfer than physical entrapment and covalent bonding, as previously mentioned, while chemical covalent bonding and electrostatic interaction bind the yeast cell to the MWCNT/PEI in this structure. Electron transfer capability is lower in the GA/[yeast/MWCNT/PEI] structure compared to the yeast/MWCNT structure because of the distinct and inferior bonding mechanism.

The air state had less of an impact on the reactivity of GA/[yeast/MWCNT/PEI] and yeast/MWCNT catalysts when the initial potential range was smaller than -0.2 V against Ag/AgCl, as shown in Figure 5. According to Wooten et al. (2014), the decrease in background current can be explained by the reduction reaction of O_2 with MWCNT, which is $O_2 + 4H_+ + 4e^- \rightarrow 2H_2O$. This signifies that the electrolyte's protons and electrons were used up in the process. Then, according to Nernst's equation [34], it caused the electrolyte's pH to shift.

According to the results, the GA/[yeast/MWCNT/PEI] catalyst was not as effective as the yeast/MWCNT catalyst when it comes to transferring electrons. To facilitate the redox reactions of NAD, FAD, and cytochrome c, and to prevent electrons from reaching the electrode surface, this transfer is crucial.

3.3. Experimental evaluation of a yeast/MWCNT catalyst using electrochemistry

The study of electron transfer rate constant (k_s) values is essential for the comprehension of MFC performance. This resulted from the implementation of Laviron's formula [35], [36]. The CV curves in Figure 6a illustrates a correlation between scan rate and current density. The value of k_s can be determined by utilizing the data presented in the Laviron graph in Figure 6b. The yeast/MWCNT catalyst had an estimated k_s of $3.51 s^{-1}$.

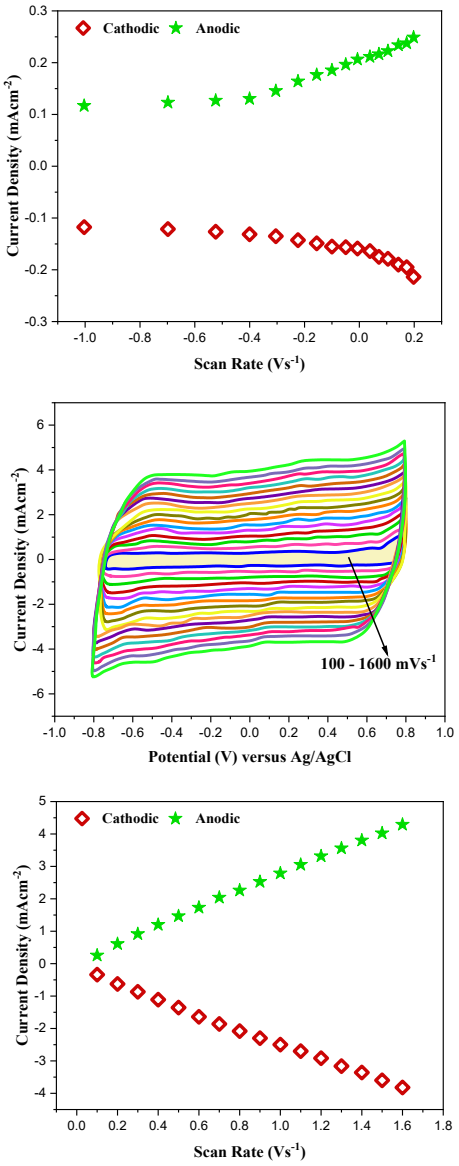

Figure 6. (a) Laviron's plot of the yeast/MWCNT catalyst's potential scan rate, (b) cyclic voltammograms measured by this rate change, and (c) a link between the yeast/MWCNT's peak current density and the potential scan rate.

The next step, after confirming yeast/MWCNT as the principal catalyst for MFC, is to identify the catalyst's rate-determining step. As shown in Figure 6c, this was achieved by keeping an eye on how the yeast/MWCNT catalyst responded to variations in potential scan rate throughout the NAD/NADH redox reaction. The experiments were conducted using a potential scanning rate ranging from 100 to 1600 mV/s and an electrolyte of 0.01 M PBS (pH 7.5), the CV tests were conducted under N_2-state [38-40]. From th results it was observed that a surface reaction-controlledyeast/MWCNT, since there was a positive link among potential scanning rate and redox reaction peak currents. Additionally, at a scanning rate of 100 mV/s, the

NAD redox process showed a 50mV discrepancy in peak potentials, ΔE_p, and an I_{pc}:I_{pa}ratio almost equal to 1. It meant that the yeast/MWCNT reaction happened in an environment where it might be undone. A formal potential of -0.657 V vs of Ag/AgCl further demonstrated that the NAD redox process was functioning properly in yeast cells of yeast/MWCNT. A formal potential was defined as the average peak potential.

In order to ensure that the yeast/MWCNT catalyst successfully transfers electrons and proton in the NAD redox process, its performance must be evaluated. To do this, it was found that the electrolyte pH correlates with the NAD redox process peak potential (Fig. 7a). With a linear fall in redox peak potential from -61 mV/pH at the anode and -69 mV/pH at the cathode as the pH between 4.1 and 8.2, the reaction between NAD and yeast/MWCNT was validated. This finding provided irrefutable evidence that the yeast/MWCNT catalyst contained viable yeast cells (Fig. 7b). Since no peak shift was noted when evaluating the pH effect of the bare MWCNT catalyst. This finding further establishes that quinone-type redox reactions do not occur with bare MWCNT. In this context, it was also established that the peaks shown in Figure 2a were caused by redox processes involving NAD, cytochrome c, and cytochrome a3, with the peak potentials of these reactions changing with the electrolyte pH.The samples were taken at various pH levels, ranging from 4.0 to 8.0. The CV tests utilized a potential scanning rate of 100 mV/s and an electrolyte of 0.01 M PBS (pH-7.4).

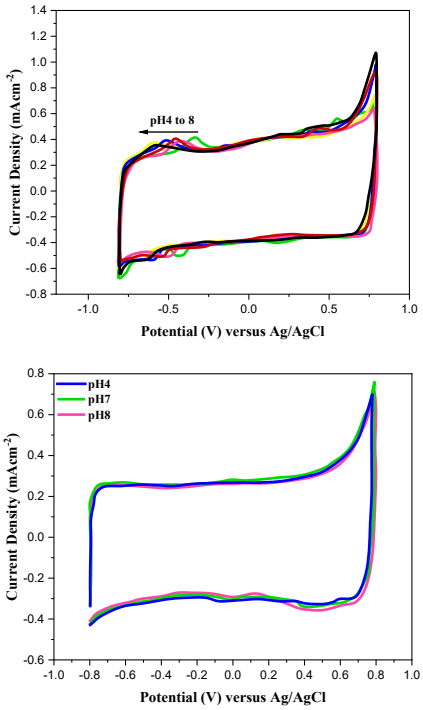

Figure 7. The cyclic voltammograms of the yeast/MWCNT and bare MWCNT

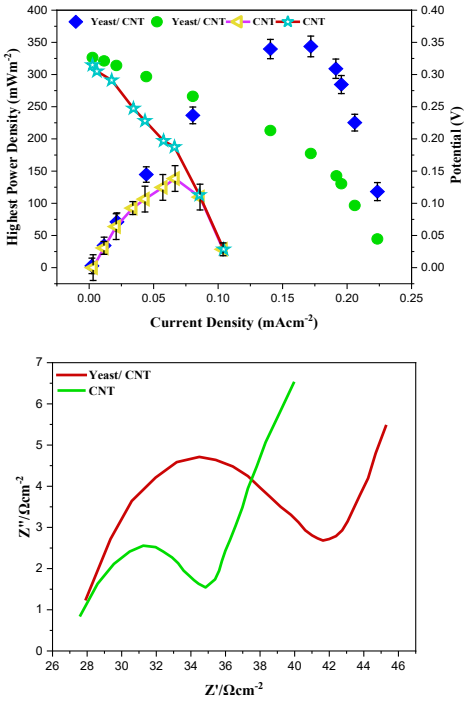

Figure 8. Microbiological anodic catalysts used in the membraneless MFCs depicted in (a) the polarizing curvature and (b) the Nyquist graph include yeast/MWCNT and bare MWCNT

3.4. Evaluation of biocatalyst-based membrane-less MFC performance and stability

This study also examined the stability and performance of membraneless MFCs using yeast/MWCNT as anodic catalysts. The polarization curves (Fig. 8a) that were measured became part of the investigation, while the enzymatic cathodic catalyst is GA/[Lac/PEI/Lac/MWCNT]. The MFC's anode chamber was supplied with a 0.04 M glucose solution via an external bottle at a flow rate of 0.1 mL· min^{-1} during the investigations. As part of the cathodic process, 100 mL/min of O_2 gas was provided. Throughout the analysis of EIS, 50 mL.min^{-1} of hydrogen gas was given to the cathode reservoir. The cathodic catalyst was a laccase-based catalyst, and previous reports on its catalytic activity and reaction selectivity were cited [34]. Triplicate measurements of the polarization curve were taken to examine the repeatability of the membraneless MFC performance. Our experiments were conducted at a pH of 7.5, the ideal environment for living microbes, even though laccase was most effective as a cathode biocatalyst at acidic conditions [35]. The greatest power density of the membrane-less MFC with the yeast/MWCNT catalyst remained368mW/m^2, as shown in Figure 8a. In order to compare and evaluate the impact of the yeast cell on the circuit's performance. In addition, polarization curve of a membrane-less MFC was also examined that utilized bare MWCNT; this MFC had an MPD of 145 mW·m^{-2}.

By comparing the polarization curves, we find that using yeast as the catalyst significantly improves the performance of membrane-less MFCs by as much as 155%, resulting in an increase in the MPD of these cells from 145 to 365 mWm^{-2}.

Evidence of no more glucose oxidation reaction can be seen by looking for a statistically significant error bar in the polarization curve. If the MFCs used similar microbe catalysts from *Saccharomyces cerevisiae* species, this MPD outperforms them even if they had a membrane. In their study on multi-feedback cells (MFCs), the scientists found that a *Saccharomyces cerevisiae* electrode coated with Reticulated Vitreous Carbon (RVC) and mediated by Neutral Red (NR) could achieve a 112 mWm^{-2} value [12]. The efficiency of graphite electrodes immobilized with *Saccharomyces cerevisiae* and thionine in micro fuel cell (MFC) studies was 71 $mW{\cdot}m^{-2}$, methylene blue (MB) served as a mediator, and the carbon felt immobilized with *Saccharomyces cerevisiae* achieved an efficiency of 353 $mW{\cdot}m^{-2}$[36].

In comparison to membraneless MFCs using other microorganism catalysts, those using yeast/MWCNT as a catalyst perform better. Attaching *Candida melibiosica* to carbon felt resulted in maximum power dissipation (MPD) values of 51 $mW{\cdot}m^{-2}$ for the two-chamber fuel cell device and 16 $mW{\cdot}m^{-2}$ for the multi-fuel cell (MFC) that used Methyl Orange (MO) as a mediator [37]. *Arxulaadeninivorans* connected to a carbon fiber cloth electrode produced a value of 68 $mW{\cdot}m^{-2}$ in a two-chambered fuel cell system [11]. On the other hand, 52 $mW{\cdot}m^{-2}$ was determined in a semicontinuous dual chamber system that contained *Geobacteraceae* according to study conducted by [37].

Nyquist curve analysis of membraneless MFCs was carried out for the purpose of comparing catalyst performance (Fig. 8b). R_s and R_{ct} were used to measure the catalysts' performance. The resistance resulting from charge transfer, including electron transfer linked to the relevant process, is denoted as R_{ct}, while the resistance resulting from the electrolyte is R_s.The statistical analysis revealed no significant difference in Rs (27~29.7 $\Omega{\cdot}cm^2$) between MFCs using bare MWCNT and yeast/MWCNT catalysts (Fig. 8b). Comparatively speaking, the MFCs varied with respect to their R_{ct} values. The MFC's R_{ct} was 16.5 $\Omega{\cdot}cm^2$ when the yeast/MWCNT catalyst was used, compared to 8.4 $\Omega{\cdot}cm^2$ when the raw MWCNT catalyst was used. Yeast, like enzymes, is not a conductive substance. Hence, the yeast/MWCNT catalyst may raise R_{ct}, which means that it does not boost electron transfer resistance [37]. The outcome was consistent with what was predicted by the polarization curve in Figure 8a.

Measurements of the MFC's MPD were repeated every two days to examine the stability of the membraneless MFC using the yeast/MWCNT catalyst (Fig. 9). The tests entailed flowing a 0.04 M glucose solution from an external bottle to the anode chamber of the MFC at a flow rate of 0.1 mL/min. The cathode reaction consumed oxygen gas at a rate of 100 mL/min.Despite our challenges in locating additional data on the durability of membraneless MFC systems using yeast cells, we were able to confirm that the MPD of these systems remained stable for up to eight days, maintaining values between 352 and 386 $mW{\cdot}m^{-2}$, which was 87% of their initial value. By observing the stability and performance of membraneless MFCs that utilized the yeast/MWCNT catalyst, as well as the reactivity of the yeast cells themselves, it was demonstrated that the catalyst made it easy for electrons to go from the cell to the outside electrode.

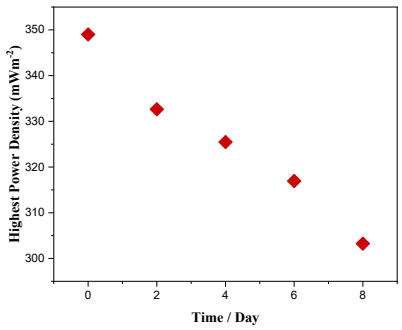

Figure 9. An analysis of the stability of yeast/MWCNT MFCs using a time-power density correlation plot.

4. CONCLUSION

A membraneless MFC that used a yeast/MWCNT catalyst was studied for its catalytic activity, stability, and performance. Accordingly, experimental evidence showed that yeast/MWCNT produced robust catalytic activities, enhanced MFC performance, and preserved suitable MFC stability. Because of their strong hydrophobic contact and covalent link (C-N bond), the results showed that the yeast/MWCNT combination was found to vebest. Another option is to use electrostatic interaction between yeast and PEI to create a unique competitive catalyst called GA/[yeast/MWCNT/PEI]. In this catalyst, GA crosslinking acts as a weak bond. Electron transport was made easier by hydrophobic contact and covalent bonding. Consequently, MFCs that used the yeast/MWCNT catalyst demonstrated remarkable stability and performance.

REFERENCES

[1] M. Christwardana and Y. Kwon, 2017, "Yeast and carbon nanotube based biocatalyst developed by synergetic effects of covalent bonding and hydrophobic interaction for performance enhancement of membraneless microbial fuel cell," *Bioresour Technol*, vol. 225, pp. 175–182. DOI:10.1016/j.biortech.2016.11.051

[2] X. Zhai, X. Liu, H. Dong, M. Lin, X. Zheng, and Q. Yang, 2024, "Implementation of cytochrome c proteins and carbon nanotubes hybrids in bioelectrodes towards bioelectrochemical systems applications," *Bioprocess Biosyst Eng*, vol. 47, no. 2, pp. 159–168. DOI:10.1007/s00449-023-02933-x

[3] M. Verma and V. Mishra, 2021, "Recent trends in upgrading the performance of yeast as electrode biocatalyst in microbial fuel cells," *Chemosphere*, vol. 284, p. 131383. DOI:10.1016/j.chemosphere.2021.131383

[4] M. N. Zafar, I. Aslam, R. Ludwig, G. Xu, and L. Gorton, 2019, "An efficient and versatile membraneless bioanode for biofuel cells based on Corynascus thermophilus cellobiose dehydrogenase," *Electrochim Acta*, vol. 295, pp. 316–324. DOI:10.1016/j.electacta.2018.10.047

[5] R. N. V. P. S. J. V. N. S. A. Sugumar Mohanasundaram Sethuraj Geetha and M. Thiruvengadam, 2024, "Evaluation of anti-corrosion potential of Datura Metel plant extract on mild steel upon sulphuric acid exposure," *Canadian*

Metallurgical Quarterly, vol. 0, no. 0, pp. 1–14. DOI:10.1080/00084433.2024.2310352

[6] M. Tawalbeh, R. Muhammad Nauman Javed, A. Al-Othman, and F. Almomani, 2022, "The novel advancements of nanomaterials in biofuel cells with a focus on electrodes' applications," Fuel, vol. 322, p. 124237. DOI:10.1016/j.fuel.2022.124237

[7] L. Addagadaet al., 2023, "Tricks and tracks in resource recovery from wastewater using bio-electrochemical systems (BES): A systematic review on recent advancements and future directions," Journal of Water Process Engineering, vol. 56, p. 104580. DOI:10.1016/j.jwpe.2023.104580

[8] Loganathan, M., Dinesh, S., Vijayan, V., Karuppusamy, T., Rajkumar, S. (2020). Investigation of mechanical behaviour on composites of Al6063 alloy with silicon, graphite and fly ash. Journal of New Materials for Electrochemical Systems, Vol. 23, No. 1, pp. 36-39. DOI: 10.14447/jnmes.v23i1.a03

[9] H. Sarma et al., 2021, "Fungal-mediated electrochemical system: Prospects, applications and challenges," Curr Res Microb Sci, vol. 2, p. 100041. DOI:10.1016/j.crmicr.2021.100041

[10] Sankar, L.P., Kamalakannan, R., Aruna, G., Meera, M.R., Vijayan, V., Sivananthan, S. (2020). Mechanical behavior and microstructure evolution of Al-5%Cu/TiC metal matrix composite. Journal of New Materials for Electrochemical Systems, Vol. 23, No. 4, pp. 252-255. DOI: 10.14447/jnmes.v23i4.a05

[11] M. Christwardana, K. J. Kim, and Y. Kwon, 2016, "Fabrication of Mediatorless/Membraneless Glucose/Oxygen Based Biofuel Cell using Biocatalysts Including Glucose Oxidase and Laccase Enzymes," Sci Rep, vol. 6, no. 1, p. 30128. DOI: 10.1038/srep30128

[12] Roseline, S., Paramasivam, V., Parameswaran, P., Antony, A.G. (2019). Evaluation of mechanical properties and stability of Al 6061 with addition of ZrO2 And Al2O3. Journal of New Materials for Electrochemical Systems, Vol. 22, No. 1, pp. 21-23. DOI: 10.14447/jnmes.v22i1.a05

[13] C. Zhao, P. Gai, R. Song, Y. Chen, J. Zhang, and J.-J. Zhu, 2017, "Nanostructured material-based biofuel cells: recent advances and future prospects," Chem Soc Rev, vol. 46, no. 5, pp. 1545–1564. DOI: 10.1039/C6CS00044D

[14] X. Xiao et al., 2019, "Tackling the Challenges of Enzymatic (Bio)Fuel Cells," Chem Rev, vol. 119, no. 16, pp. 9509–9558. DOI:10.1021/acs.chemrev.9b00115

[15] E. Serag, A. El-Maghraby, and A. El Nemr, 2022, "Recent developments in the application of carbon-based nanomaterials in implantable and wearable enzyme-biofuel cells," Carbon Letters, vol. 32, no. 2, pp. 395–412. DOI:10.1007/s42823-021-00299-2

[16] A. Sekrecka-Belniak and R. Toczyłowska-Mamińska, 2018, "Fungi-Based Microbial Fuel Cells," Energies (Basel), vol. 11, no. 10. DOI: 10.3390/en11102827

[17] M. Christwardana, 2017, "Combination of physico-chemical entrapment and crosslinking of low activity laccase-based biocathode on carboxylated carbon nanotube for increasing biofuel cell performance," Enzyme Microb Technol, vol. 106, pp. 1–10. DOI:10.1016/j.enzmictec.2017.06.012

[18] K. D. Z. Duarte and Y. Kwon, 2020, "Enhanced extracellular electron transfer of yeast-based microbial fuel cells via one pot substrate-bound growth iron-manganese oxide nanoflowers," J Power Sources, vol. 474, p. 228496. DOI:10.1016/j.jpowsour.2020.228496

[19] B. K. Udaya and B. P. Devadas, 2021, "Carbon Nanomaterials for Biofuel Cells," Biofuel Cells: Materials and Challenges, pp. 171–217. DOI:10.1002/9781119725008.ch7

[20] I. Gal, O. Schlesinger, L. Amir, and L. Alfonta, 2016, "Yeast surface display of dehydrogenases in microbial fuel-cells," Bioelectrochemistry, vol. 112, pp. 53–60. DOI:10.1016/j.bioelechem.2016.07.006

[21] P. Bollella and E. Katz, 2020, "Chapter Ten - Bioelectrocatalysis at carbon nanotubes," in Nanoarmoring of Enzymes with Carbon Nanotubes and Magnetic Nanoparticles, vol. 630, C. V Kumar, Ed., in Methods in Enzymology, vol. 630. , Academic Press, 2020, pp. 215–247. DOI:10.1016/bs.mie.2019.10.012

[22] M. A. Ali et al., 2022, "Metal-free, low-cost, and high-performance membraneless ethanol fuel cell," J Power Sources, vol. 551, p. 232164. DOI:10.1016/j.jpowsour.2022.232164

[23] Md. T. Noori, M. M. Ghangrekar, C. K. Mukherjee, and B. Min, 2019, "Biofouling effects on the performance of microbial fuel cells and recent advances in biotechnological and chemical strategies for mitigation," Biotechnol Adv, vol. 37, no. 8, p. 107420. DOI:10.1016/j.biotechadv.2019.107420

[24] A. J. Gross, M. Holzinger, and S. Cosnier, 2018, "Buckypaper bioelectrodes: Emerging materials for implantable and wearable biofuel cells," Energy Environ Sci, vol. 11, no. 7, pp. 1670–1687. DOI: 10.1039/c8ee00330kf

[25] J. Kim, H. Jia, and P. Wang, 2006 "Challenges in biocatalysis for enzyme-based biofuel cells," Biotechnol Adv, vol. 24, no. 3, pp. 296–308. DOI:10.1016/j.biotechadv.2005.11.006

[26] P. Ó Conghaile et al., 2016, "Fully Enzymatic MembranelessGlucose|Oxygen Fuel Cell That Provides 0.275 mA cm–2 in 5 mM Glucose, Operates in Human Physiological Solutions, and Powers Transmission of Sensing Data," Anal Chem, vol. 88, no. 4, pp. 2156–2163. DOI:doi.org/10.1021/acs.analchem.5b03745

[27] B. Ghosh, R. Saha, D. Bhattacharya, and M. Mukhopadhyay,2019, "Laccase and its source of sustainability in an enzymatic biofuel cell," Bioresour Technol Rep, vol. 6, pp. 268–278. DOI:10.1016/j.biteb.2019.03.013

[28] W. Wu et al., 2019, "Controlled Layer-By-Layer Deposition of Carbon Nanotubes on Electrodes for Microbial Fuel Cells," Energies (Basel), vol. 12, no. 3. Doi:10.3390/en12030363

[29] J. Ma et al., 2023, "Progress on anodic modification materials and future development directions in microbial

fuel cells," J Power Sources, vol. 556, p. 232486. Doi:10.1016/j.jpowsour.2022.232486

[30] J. L. Zhang, Y. H. Wang, K. Huang, K. J. Huang, H. Jiang, and X. M. Wang, 2021, "Enzyme-based biofuel cells for biosensors and in vivo power supply," Nano Energy, vol. 84, p. 105853. Doi: 10.1016/j.nanoen.2021.105853

[31] K. Chansaenpaket al., 2021, "Development of a Sensitive Self-Powered Glucose Biosensor Based on an Enzymatic Biofuel Cell," Biosensors (Basel), vol. 11, no. 1. Doi:10.3390/bios11010016

[32] Y. Hui, X. Ma, R. Cai, and S. D. Minteer, 2021, "Three-dimensional glucose/oxygen biofuel cells based on enzymes embedded in tetrabutylammonium modified nafion," Journal of Electrochemical Energy Conversion and Storage, vol. 18, no. 4, p. 041004. Doi : 10.1115/1.4049926

[33] K. Dutta and P. P. Kundu, 2014, "A Review on Aromatic Conducting Polymers-Based Catalyst Supporting Matrices for Application in Microbial Fuel Cells," Polymer Reviews, vol. 54, no. 3, pp. 401–435. Doi:10.1080/15583724.2014.881372

[34] K. Hyun, S. Kang, J. Kim, and Y. Kwon, 2020, "New Biocatalyst Including a 4-Nitrobenzoic Acid Mediator Embedded by the Cross-Linking of Chitosan and Genipin and Its Use in an Energy Device," ACS Appl Mater Interfaces, vol. 12, no. 20, pp. 23635–23643. Doi: 10.1021/acsami.0c05564

[35] P. Rafighiet al., 2022, "A novel membraneless β-glucan/O2 enzymatic fuel cell based on β-glucosidase (RmBgl3B)/pyranose dehydrogenase (AmPDH) co-immobilized onto buckypaper electrode," Bioelectrochemistry, vol. 148, p. 108254.doi:10.1016/j.bioelechem.2022.108254

[36] S. Singh, P. K. Bairagi, and N. Verma, 2018 "Candle soot-derived carbon nanoparticles: An inexpensive and efficient electrode for microbial fuel cells," Electrochim Acta, vol. 264, pp. 119–127. Doi:10.1016/j.electacta.2018.01.110

[37] A. Sharma, G. Singh, and S. K. Arya, 2021, "Biofuel cell nanodevices," Int J Hydrogen Energy, vol. 46, no. 4, pp. 3270–3288. Doi:10.1016/j.ijhydene.2020.02.164

[38] S.Dinesh, A.Godwin Antony, S.Karuppusamy, V.Vijayan and B.Suresh Kumar, 2016. Experimental investigation and optimization of machining parameters in CNC turning operation of duplex stainless steel. Asian Journal of 2Research in Social Sciences and Humanities 6,pp. 179-195. Doi:10.5958/2249-7315.2016.01006.6

[39] S.Dinesh, A.Godwin Antony, K.Rajaguru and V.Vijayan. 2016. Investigation and Prediction of material removal rate and surface roughness in CNC turning of EN24 alloy steel, Asian Journal of Research in Social Sciences and Humanities , vol 6 (8) 849—863. DOI:10.5958/2249-7315.2016.00654.7

[40] T.Tamizharasan, N.Senthil Kumar, V.Selvkumar, S.Dinesh, 2019. Taguchi's Methodology of optimizing turning parameters over chip thickness ratio in machining PM AMMC, SN Appl. Sci. 1: 160., Springer Publishers. Doi:10.1007/s42452-019-0170-8